ELSEVIER

International Journal of Mass Spectrometry 188 (1999) 39–52

International Journal of Mass Spectrometry

Charge-remote molecular hydrogen removal in protonated and alkali-cationized long-chain fatty acid esters upon cesium ion bombardment

L. Huysmans, L. Nizigiyimana, H. Van den Heuvel, M. Claeys*

University of Antwerp (UIA), Department of Pharmaceutical Sciences, Universiteitsplein 1, B-2610 Antwerp, Belgium

Received 25 May 1998; accepted 11 September 1998

Abstract

The mass spectral behavior of cationized saturated fatty acid derivatives has been studied in order to gain insight into the loss of molecular hydrogen during cesium ion bombardment. It is shown that molecular hydrogen and hydrogen radical loss occurs for protonated and alkali (Li^+/Na^+)-cationized fatty acid methyl esters as well as for protonated acylcarnitines and that molecular hydrogen loss is dependent upon the acyl chain length. Investigation of ion structures by collision-induced dissociation tandem mass spectrometry indicates that in the case of alkali-cationization a hydrogen radical is lost from all positions of the saturated acyl chain, whereas in the case of protonated molecules a hydrogen radical is predominantly eliminated from the protonated ester group. For the primary reaction of the dehydrogenation chemistry, an ion-beam-induced excitation of a cationized molecule is proposed, yielding a diradical species that gives rise to an intermolecular reaction with a neutral analyte molecule. Subsequent cationization of the neutral [M–H_2] species formed in this primary reaction leads to the formation of the satellite ion at m/z values 2 u lower compared to the cationized molecule. (Int J Mass Spectrom 188 (1999) 39–52) © 1999 Elsevier Science B.V.

Keywords: FAB/LSIMS; Beam-induced processes; Charge-remote fragmentation; Collision-induced dissociation

1. Introduction

Liquid secondary ion (LSI) or fast atom bombardment (FAB) mass spectrometry has been and still is widely used for the analysis of phospholipids and fatty acid derivatives. In previous investigations on protonated and lithium-cationized fatty acid derivatives we noted that the $[M + H]^+$ or $[M + Li]^+$ ions are accompanied by significant ions at masses 1 and 2 u lower [1]. It was also found that the abundance of these satellite ions is dependent upon the chain length. A similar behavior was observed for the molecular cations of *n*-alkyltriphenylphosphonium salts containing long-chain alkyl groups [2].

The phenomenon of molecular hydrogen loss from protonated diacylphosphatidylcholines under FAB conditions, which is a drawback in the analysis because of possible confusion of the dehydrogenated ion with more highly unsaturated species, has been reported by Fenwick et al. [3] and Allmaier et al. [4]. The loss of molecular hydrogen from molecular ions

* Corresponding author.

We are delighted to dedicate this article to Brian Green in recognition for the generous help he provided during our various visits to Manchester.

PII S1387-3806(98)14206-9

($M^{+\bullet}$) has also been observed for field desorption (FD) of saturated hydrocarbons, and has been investigated in detail by Heine and Geddes [5], and, more recently, by Klesper and Röllgen [6]. The phenomenon was shown to be strongly dependent upon the field strength and the amount of sample applied onto the emitter. As to the mechanism of molecular hydrogen loss, a field-induced proton transfer from a molecular ion to a neighbouring molecule was suggested yielding a $[M–H]^+$ ion and a $[M–H]^\bullet$ radical after elimination of molecular hydrogen, which in secondary reactions form an alkene ion or a dimer ion [6]. With respect to molecular hydrogen loss from protonated diacylphosphatidylcholines during FAB, it was presumed that the glycerol backbone is the site of the loss, but no mechanism was formulated [3]. In the present study, we have investigated the phenomenon of molecular hydrogen loss during LSI mass spectrometry for protonated and alkali (Li^+/Na^+)-cationized fatty acid methyl esters with a varying acyl chain length. We demonstrate that this phenomenon becomes more pronounced with a longer ester acyl chain and that the introduction of (an) unsaturation(s) and branching in the acyl chain has an inhibitory effect.

In addition, the ion structures of alkali-cationized and protonated methyl lignocerate that lost $H^\bullet$ or H_2 have been examined by using collision-induced dissociation (CID) in order to obtain insight in the mechanism of molecular hydrogen removal during cesium ion bombardment. In previous studies $M^{+\bullet}$ and $[M–H]^+$ ion formation in FAB has been compared to corresponding features in chemical ionization (CI) and electron impact (EI) spectra and presented as evidence of gas-phase ionization processes being important in FAB [7–9]. However, this mechanism was questioned by Paul et al. [10,11], who examined a series of cyclic acetals and derivatized monosaccharides and concluded that fast atom/ion-beam-induced processes are likely responsible for the observed mass spectral characteristics. It was demonstrated that in CI, ions of the type $[M + H]^+$ are predominant, whereas $[M–H]^+$ ions are observed as important species in EI and FAB [10]. On the basis of this result and available gas phase hydride ion affinities, the dominant $[M–H]^+$ ions in FAB could not be explained in gas-phase terms and, therefore, a condensed phase ionization model was employed. To gain further information on the condensed phase processes involved in $[M–H]^+$ formation in FAB, the samples were analyzed by electrospray ionization (ESI), because ESI is believed to reflect predominantly condensed phase equilibrium processes [11]. The absence of $[M–H]^+$ ions in ESI suggested that these equilibrium processes are not responsible for hydride abstraction in FAB and that processes other than the preformation of ions in solution have to be invoked. Fast atom/ion-beam-induced processes have thus been considered the most likely origin of $[M–H]^+$ ions in FAB of cyclic acetals. In the present study, we advance arguments in favour of ion-beam-induced processes being important during liquid secondary ionization mass spectrometry (LSIMS) of alkali metal-cationized fatty acid methyl esters.

2. Experimental

2.1. Materials

All samples listed in Table 1, except the acylcarnitines, were purchased from Sigma (St. Louis, MO) or from Applied Science (State College, PA). The acylcarnitines were available from a previous study by Van Bocxlaer et al. [12].

2.2. Derivatization

The methyl ester derivatives of the unsaturated fatty acids, stearic acid, and phytanic acid were prepared by dissolving the fatty acids in dichloromethane and adding an excess of diazomethane. After reacting at room temperature for 15 min, the solvent mixture was evaporated under nitrogen.

2.3. Mass spectrometry

The LSI and EI mass spectra were obtained on a VG70SEQ hybrid mass spectrometer (Micromass, Manchester, UK) with EBqQ configuration equipped with both LSI and EI ionization sources. For record-

Table 1
List of samples

R_1-COO-R_2			
Fatty acid methyl esters		Acylcarnitines	
R_2 = —CH_3		R_2 = —CH(CH_2—COO^-)(CH_2—$N^+(CH_3)_3$)	
Compound	R_1	Compound	R_1
Saturated			
1	$C_{15}H_{31}$	12	C_6H_{13}
2	$C_{17}H_{35}$	13	C_7H_{15}
3	$C_{19}H_{39}$	14	C_8H_{17}
4	$C_{23}H_{47}$	15	C_9H_{19}
5	$C_{25}H_{51}$	16	$C_{10}H_{21}$
6	$C_{27}H_{55}$	17	$C_{11}H_{23}$
7	$C_{29}H_{59}$	18	$C_{12}H_{25}$
Unsaturated			
8	$C_{17}H_{33}$	19	$C_{14}H_{29}$
9	$C_{17}H_{31}$	20	$C_{16}H_{33}$
10	$C_{17}H_{29}$	21	$C_{18}H_{37}$
Branched			
11	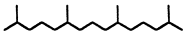		

ing LSI mass spectra cesium ions with an impact energy of approximately 18 keV (unless stated otherwise) and a beam flux of 0.3 μA were used as the ionization beam. The accelerating voltage in the source was 8 kV. The fatty acids were dissolved in dichloromethane (2 mg ml^{-1}) and 1 μL of the solution was mixed with 2 μL of the liquid matrix on the stainless-steel probe tip. As liquid matrices, *m*-nitrobenzylalcohol (*m*-NBA) and *m*-NBA saturated with LiI (*m*-NBA + Li) or NaI (*m*-NBA + Na) were used to produce $[M + H]^+$, $[M + Li]^+$, and $[M + Na]^+$ precursor ions, respectively. The acylcarnitines were dissolved in methanol (10 $\mu g\ \mu L^{-1}$) and 1 μL of the solution was mixed with 2 μL of glycerol on the stainless-steel probe tip.

The EI mass spectra were obtained by direct inlet introduction with a standard EI source. The source was operated at 200 μA trap current and an electron energy of 70 eV. Mass spectra were continuously acquired at a scan rate of 3 s/decade as the probe temperature increased from 30 °C to ~500 °C with a heating rate of 100 °C/min.

The product ion spectra were obtained on an AutoSpec orthogonal acceleration time-of-flight (oaTof) mass spectrometer (Micromass, Manchester, UK), which is a hybrid tandem instrument comprising a standard AutoSpec of EBE geometry (MS1) and an orthogonal time-of-flight mass analyzer (MS2), and is equipped with a cesium ion source. The ion gun was operated at an anode potential of 25 kV and the accelerating voltage in the source was 8 kV. For acquiring high-energy CID spectra, xenon was employed as collision gas at a pressure sufficient to attenuate the parent ion beam by 75%. MS1 was operated at a resolution of 1500. The collision energy was 800 eV [laboratory frame of reference (E_{lab})]. Product ions were mass analyzed by MS2 and detected on a multichannel plate. To record low-energy CID spectra, helium was used as collision gas. All the other circumstances remained the same.

The first-order mass spectrometric data obtained for the protonated and alkali-cationized molecules were evaluated as ion intensity ratios. To compare the desorption behavior of the different alkali-cationized fatty acid methyl esters, an abundant *m*-NBA cluster ion was chosen.

Isotope corrections were carried out for ^{13}C and ^6Li. The relative abundance of ^6Li was found to be 5.5% from detailed interpretation of the $(LiI)I^-$ ion cluster in the negative FAB mass spectrum of LiI.

2.4. Ion nomenclature

The nomenclature for the fragmentation of fatty acid molecule ions in CID reactions introduced by Griffiths et al. [13] and modified by Claeys et al. [14] has been followed. For clarity, the rules relevant to this study are briefly summarized: (1) the italicized capital letters *C*, *H*, and *A* are used to describe the nature of the bond broken with the charge retained on the carboxylate group (*C* refers to a bond in a saturated part, *H* to a homoallylic bond, and *A* to an allylic bond) (Scheme 1); (2) a subscript to the right of the letter indicates the number of carbon atoms remaining in the fatty acyl part, e.g. C_n, and; (3) a prime to the left of the letter indicates that the product ion is deficient in one hydrogen compared with that product ion that would be formed by a homolytic

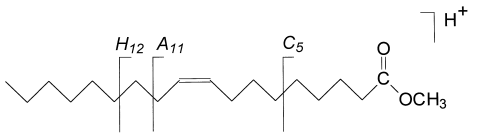

Scheme 1. Nomenclature for the fragmentation of fatty acid molecule ions in CID reactions.

fragmentation at the same point in the precursor molecule ion.

The *C* ions are formed by cleavage of a C–C bond and can be regarded as odd-electron (OE) ions. The terminally unsaturated ions $'C_n$ are generated by C–H cleavage at various positions in the acyl chain and subsequent radical-induced C–C cleavage, and correspond to even-electron (EE) ions.

The term "charge-remote" fragmentation is used in this study to refer to fragmentation reactions in the acyl chain corresponding to formal losses of elements of alkanes and to alkyl losses. However, it is pointed out that in view of new insights in their mechanism, these reactions can be regarded as "radical induced" [15] and that the term "charge remote" may be misleading.

3. Results and discussion

3.1. LSIMS of fatty acid methyl esters

3.1.1. $[M + Li]^+$ ions

Fig. 1 illustrates the LSI mass spectrum obtained for Li^+-cationized methyl lignocerate (**4**). The base peak corresponds to the lithiated molecule $[M + Li]^+$, but in addition relatively abundant $[M + Li–H]^{+\bullet}$ and $[M + Li–H_2]^+$ ions are present at *m*/*z* 388 and *m*/*z* 387, respectively. Similar spectra were obtained for the other saturated fatty acid methyl esters mentioned in Table 1. All these spectra show the formation of ions at *m*/*z* values 1 and 2 u lower than

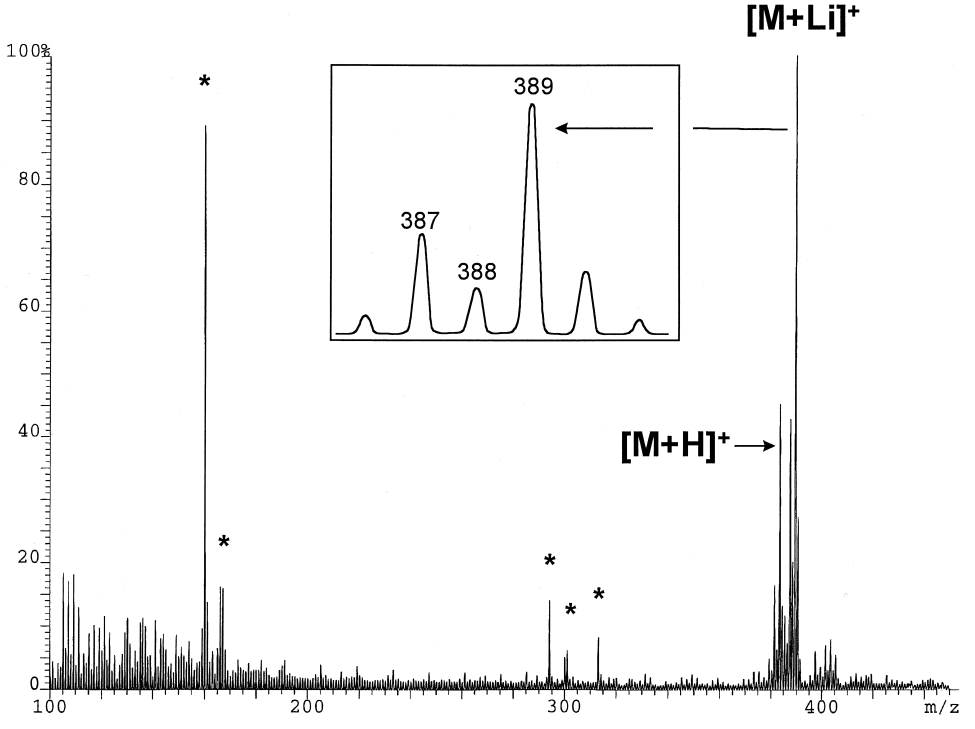

Fig. 1. LSI mass spectrum obtained for methyl lignocerate by using *m*-NBA saturated with LiI. The peaks marked with an asterisk are because of the matrix. A detail of the $[M + Li]^+$ region is given in the inset.

Table 2
Abundances of the satellite ions formed by loss of H_2 relative to the alkali (Li/Na)-cationized molecules of fatty acid methyl esters (sample loading: 2 μg) and the intensity ratio of the cationized molecules relative to a *m*-NBA cluster ion for the saturated compounds

Compound	$[M + Li–H_2]^+/[M + Li]^+$ (%)	$[M + Li]^+/[m/z\ 160]$	$[M + Na–H_2]^+/[M + Na]^+$ (%)	$[M + Na]^+/[m/z\ 176]$
Saturated				
1	7.3	1.01 ± 0.06	5.3	0.20 ± 0.06
2	13.1	5.02 ± 0.48	3.7	0.97 ± 0.08
3	21.7	8.16 ± 0.81	13.5	5.40 ± 0.46
4	34.9	0.63 ± 0.06	36.5	0.40 ± 0.13
5	48.7	0.50 ± 0.13	46.1	0.40 ± 0.17
6	69.8	0.16 ± 0.06	73.1	0.14 ± 0.04
7	92.2	0.10 ± 0.009	86.1	0.07 ± 0.01
Unsaturated				
8	10.0			
9	6.6			
10	7.2			
Branched				
11	14.6			

the $[M + Li]^+$ adduct ions. After isotope corrections a clear trend was observed for the formation of the $[M + Li–H_2]^+$ ion, but not for the $[M + Li–H]^{+\bullet}$ ion. Table 2 summarizes the signal intensities of the ions because of the loss of molecular hydrogen relative to the $[M + Li]^+$ signals as measured from the LSI mass spectra. The results obtained for saturated fatty acid methyl esters demonstrate that the abundance of the satellite ion increases significantly with the length of the acyl chain.

Another parameter of interest is the $[M + Li]^+$/[*m*-NBA cluster ion] ratio, which can be regarded as a measure of the $[M + Li]^+$ ion yield. The data summarized in Table 2 show that the $[M + Li]^+/[m/z\ 160]$ ratio reveals a maximum for the C_{20} fatty acid methyl ester, but decreases considerably as the chain length further increases.

In addition to the influence of the chain length, the effect of unsaturation in the acyl chain was also examined. Comparison of the LSIMS data obtained for methyl stearate (**2**), methyl oleate (**8**), methyl linoleate (**9**), and methyl α-linolenate (**10**) shows that the introduction of an unsaturation appears to inhibit the removal of molecular hydrogen (Table 2). This inhibition becomes more pronounced as the degree of unsaturation increases. Methyl linoleate yields a $[M + Li–H_2]^+$ ion that is only half as abundant as that derived from the saturated product. The same effect was observed if a compound with double bonds was admixed with a saturated compound. In a 1:1 mixture of methyl lignocerate (**4**) and methyl α-linolenate (**10**), the $[M + Li–H_2]^+/[M + Li]^+$ abundance ratio amounts to 29%, whereas with pure methyl lignocerate the ratio is 35%. In the latter experiment methyl lignocerate was used instead of methyl stearate, because this fatty acid showed less interference with the peaks of the unsaturated sample.

In further experiments the introduction of branching was investigated. The spectra were recorded for the methyl ester of a branched compound, namely, phytanic acid (**11**), and its linear homolog, methyl arachidate (**3**). It was found that the abundance of the ion because of H_2 loss decreases significantly in the case of the branched compound compared to the linear product (Table 2). Hence, the presence of double bonds as well as branching appears to inhibit the reaction that yields this ion.

Another factor that might influence the abundance of the satellite ion is the amount of sample loaded on the probe tip. The employed sample loadings were changed from 0.1 to 4 μg for the compounds methyl stearate (**2**) and methyl lignocerate (**4**). The results obtained for methyl stearate (not shown) revealed no significant effect of the sample quantity on the abundance of the satellite ion. On the other hand, the spectra of methyl lignocerate for which the cationized

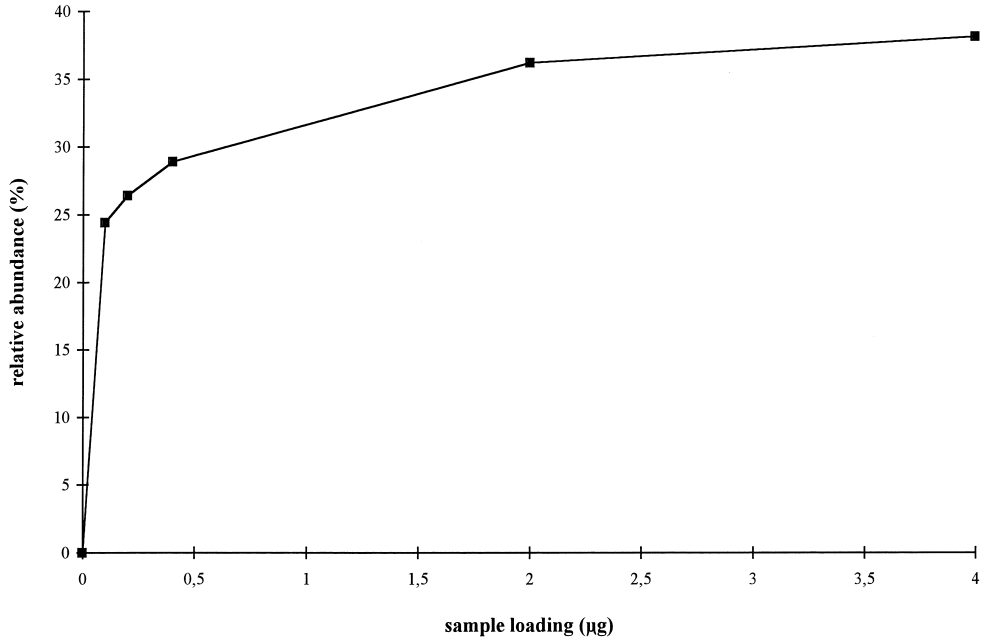

Fig. 2. Influence of quantity of compound **4** on abundance of the $[M + Li–H_2]^+$ ion relative to Li^+-cationized molecules.

molecules show a decreased desorption relative to the lower methyl stearate homolog, illustrate a tendency of an increased loss of H_2 from the $[M + Li]^+$ ion as the amount of sample increases (Fig. 2).

Finally, the impact energy of the Cs^+ ions was varied to study a possible effect on the removal of molecular hydrogen from the $[M + Li]^+$ adduct ions. The impact energy of the ion beam was decreased from 18 to 2 keV, approximately. Only above 6 keV Li^+-cationized molecules were detected and between 6 and 18 keV, no obvious effect of the Cs^+ ion impact energy on the abundance of the satellite ion was observed.

The phenomenon of molecular hydrogen loss from the $M^{+\bullet}$ ion has been examined in detail for long-chain hydrocarbons under FD conditions, where it was found to be dependent upon the chain length, the field strength, and the amount of sample applied onto the emitter. The addition of a polyunsaturated homolog gave rise to a decreased loss of H_2 [5,6]. These results are similar to ours obtained in LSIMS for Li^+-cationized fatty acid methyl esters. However, in contrast to LSIMS, branching resulted in an enhanced loss of molecular hydrogen from M^+ ions of long-chain hydrocarbons under FD conditions. Furthermore, it is worth mentioning that in LSIMS a relatively abundant ion at a m/z value 4 u lower than the $[M + Li]^+$ adduct ion is noticed comparable to observations in FD for the $M^{+\bullet}$ ions of long-chain hydrocarbons [6]. The formation of this ion also becomes more pronounced as the chain length increases.

3.1.2. $[M + Na]^+$ ions

In a following series of experiments we examined the phenomenon of $H^\bullet$ and H_2 loss for Na^+-cationized saturated fatty acid methyl esters. Again, only the $[M + Na–H_2]^+$ ions showed an obvious tendency after isotope corrections. The relative abundances of the $[M + Na–H_2]^+$ ions relative to $[M + Na]^+$ adduct ions are given in Table 2. With the exception of methyl stearate (**2**), these results show a similar trend as observed for the lithiated compounds suggesting that a similar mechanism is involved in the loss of molecular hydrogen. Furthermore, it is worth noting that the $[M + Na]^+$/[*m*-NBA cluster ion] ratio shows

Table 3
Abundances of the satellite ions formed by loss of H_2 relative to the protonated molecules of saturated fatty acid methyl esters (sample loading: 2 μg) and acylcarnitines (sample loading: 10 μg)

Compound	$[M + H–H_2]^+/[M + H]^+$ (%)
1	11.3
2	10.7
3	14.9
4	17.3
5	16.1
12	1.5
13	2.0
14	2.3
15	2.8
16	2.6
17	3.1
18	3.4
19	4.4
20	5.7
21	7.8

a profile comparable to that observed for the Li^+-cationized molecules. The $[M + Na]^+/[m/z\ 176]$ ratio maximizes for the C_{20} fatty acid methyl ester and further drops significantly for the higher homologs.

3.1.3. $[M + H]^+$ ions

For the first five saturated fatty acid methyl esters mentioned in Table 1, the tendency to lose molecular hydrogen from protonated molecules was evaluated. It is known that $[M + Li]^+$ adduct ions have a more stable charge centre than $[M + H]^+$ ions and that the fragmentation of these lithiated molecular species can be significantly different from that of protonated species [16]. In the present study a major difference is also observed between the Li^+/Na^+-cationized ions and the protonated molecules with respect to the loss of H_2: the tendency of removal of H_2 is much less pronounced in the case of $[M + H]^+$ ions (Table 3). These results suggest that compared to the alkali-cationized molecules, another mechanism may operate in the formation of the satellite ions.

Molecular hydrogen loss from protonated phospholipids under FAB conditions has been reported by Fenwick et al. [3] and by Allmaier et al. [4]. This H_2 loss creates possible confusion of the dehydrogenated ion with a more highly unsaturated species, especially in mixture analysis. In these studies, it was presumed that the glycerol backbone is the site of dehydrogenation and that this process may take place during the desorption/ionization process. Allmaier et al. [4] observed that the intensity of the $[M + H–H_2]^+$ ions was affected by the matrix used. In the case of phospholipids, the formation of $[M + H–H_2]^+$ ions was lower by using *m*-NBA as a liquid matrix compared to glycerol.

3.1.4. LSIMS of acylcarnitines

In a previous study concerning the characterization of acylcarnitines by FAB mass spectrometry, we noted that the protonated molecules were accompanied by ions at m/z values 2 u lower corresponding to the loss of molecular hydrogen [12]. An extended series of acylcarnitines, which are shown in Table 1, were examined to evaluate whether there is a relationship between the acyl chain length and the extent of H_2 loss. The results (Table 3) indicate that elongation of the acyl part of the acylcarnitines gives rise to an enhanced loss of molecular hydrogen. However, the increasing trend observed for these protonated compounds to lose molecular hydrogen is much less pronounced than that obtained for the Li^+/Na^+-cationized fatty acid methyl ester derivatives. These results indicate that molecular hydrogen removal during LSIMS is compound dependent.

4. CID investigation of ion structures

4.1. $[M + Li–1]^{+\bullet}$ and $[M + Li–2]^+$ ion structures

High-energy CID spectra of lithiated methyl lignocerate (**4**) were acquired at a laboratory collision energy of 800 eV (E_{lab}), which corresponds to a centre of mass collision energy (E_{com}) of 200 eV when xenon is employed as collision gas. High-energy CID reactions are usually thought to occur when the E_{com} exceeds 25 eV [17]. Fig. 3 shows the high-energy CID spectrum obtained for the $[M + Li]^+$ ion of methyl lignocerate. As expected, the $[M + Li]^+$ adduct ion, which contains a stable site of charge, shows charge-remote fragmentation (CRF) of the fatty acid chain,

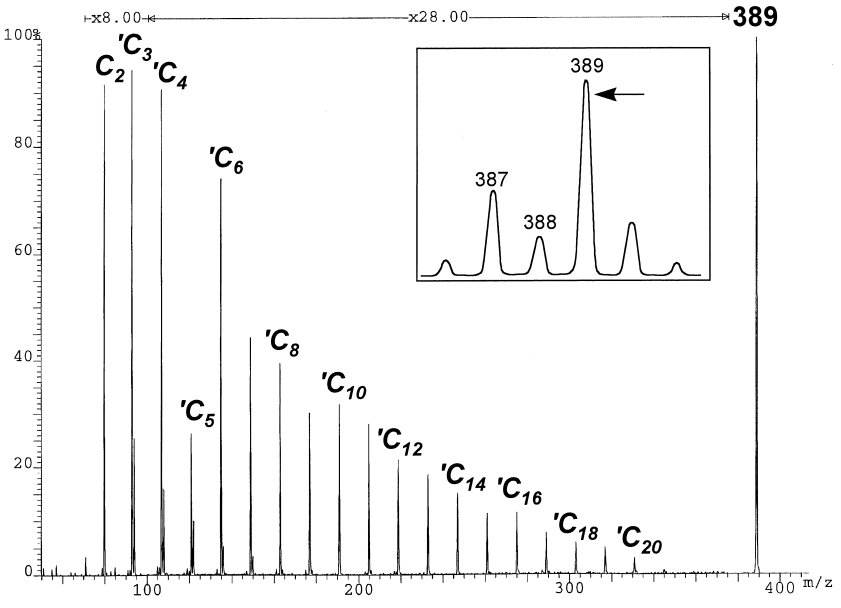

Fig. 3. High-energy CID spectrum of the methyl lignocerate $[M + Li]^+$ ion (E_{com} 200 eV). A detail of the LSI mass spectrum is given in the inset.

giving rise to a very clear homologous series of $'C_x$ ions. It is worth noting that this series of charge-remote product ions appears to continue in the lower mass range and terminates with an ion at m/z 80 that corresponds to an odd-electron (OE) ion formed by cleavage of the C2–C3 bond. The decreased abundance of the $'C_5$ ion at m/z 121 is difficult to rationalize by a mechanism involving a concerted 1,4-elimination of hydrogen as proposed by Jensen and co-workers [18]. The formation of the OE ion at m/z 80 and the decreased formation of the ion at m/z 121 ($'C_5$) can more readily be explained by competing radical reactions, starting with homolytic C–H cleavage at the C4 position [19]. The latter mechanism involving C–H cleavage was originally proposed in a study by Claeys and Van den Heuvel [20] on the CRF behavior of Li^+-cationized long-chain alkenyl salicylic acids and has been further elaborated in a recent investigation by Claeys et al. [15]. Briefly, in the latter study an alternate mechanism has been formulated for high-energy CID processes of Li^+-cationized fatty acid esters, involving the formation of a transient diradical located in the ester carbonyl group that is the trigger for C–H and C–C cleavage reactions in the fatty acid acyl chain.

In subsequent experiments, the fragmentation behavior of the $[M + Li–H]^{+\bullet}$ ion of methyl lignocerate was examined by using both high- and low-energy CID. The low-energy CID spectra were acquired by using helium as collision gas at 800 eV E_{lab} that corresponds to 8 eV E_{com}. The low-energy CID spectrum of the $[M + Li–H]^{+\bullet}$ ion is illustrated in Fig. 4. It is worth noting that the same homologous series of $'C$ ions and the C_2 ion are noted as observed in the high-energy CID spectrum of the corresponding $[M + Li]^+$ ion. These results indicate that hydrogen radical loss during LSIMS occurred at all positions of the acyl chain and that the subsequent radical-induced fragmentation corresponds to a low-energy CID process. The abundance differences observed for the various $'C$ ions further suggest that hydrogen radical removal under LSIMS conditions from the more charge-proximate positions appears to be favoured.

The high-energy CID spectrum of the $[M + Li–H]^{+\bullet}$ ion of methyl lignocerate (not shown) reveals the same ions as those noted for low-energy CID with

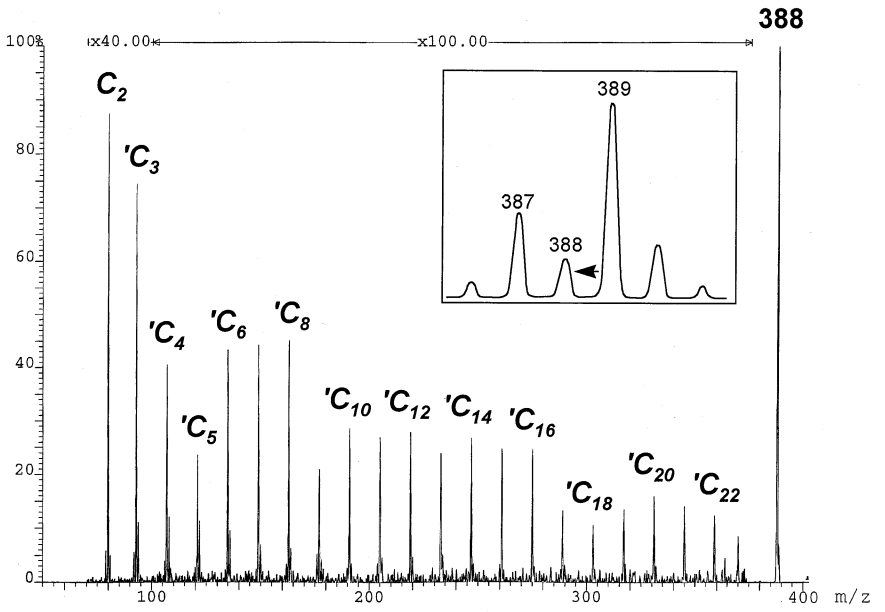

Fig. 4. Low-energy CID spectrum of the methyl lignocerate $[M + Li–H]^{+\bullet}$ ion (E_{com} 8 eV). A detail of the LSI mass spectrum is given in the inset.

similar abundances. However, compared to the low-energy CID spectrum, this spectrum is more complicated because ions due to high-energy CID of the $[M + {}^{6}Li]^{+}$ isotopic ion are also present in the spectrum at a mass 1 u lower than those of the $'C_x$ ions. The absence of these satellite ions (Fig. 4) confirms that the observed fragmentation under low-energy CID conditions is only because of fragmentation of the $[M + Li–1]^{+\bullet}$ ion and does not originate from the $[M + {}^{6}Li]^{+}$ isotopic ion. Hence, the applied E_{com} (8 eV) was not sufficient to induce C–H cleavage, which is a product-determining step in CRF reactions according to Claeys et al. [14], but was clearly high enough for radical-induced fragmentation in the $[M + Li–H]^{+\bullet}$ ion.

Because of the indiscriminate loss of a hydrogen radical all along the chain it is logical to propose that the removal of molecular hydrogen by the energetic cesium ion beam also occurs at random positions in the acyl chain. This loss of molecular hydrogen results in the formation of $[M + Li–2]^{+}$ ions that correspond to a mixture of monounsaturated fatty acid ions containing the unsaturation at all possible positions of the acyl chain. As expected, high-energy CID conditions were required to observe CRF product ions for the $[M + Li–H_2]^{+}$ ion of methyl lignocerate (Fig. 5). Because the precursor ion is unsaturated by loss of molecular hydrogen, the main cleavage pathways are induced by the reactive allylic sites and subsequently result in $'H_x$ ions and $'A_x$ type ions containing one or two double bonds. Deuterium labelling experiments revealed that the formation of the monounsaturated $'A_x$ ions occurs predominantly by a direct allylic C–C cleavage [14]. The high-energy CID $[M + Li–H_2]^{+}$ spectrum illustrates the formation of an extensive series of doubly unsaturated $'A_x/'H_x$ ions, indicating that the position of the double bond is random. Furthermore, it is worth noting that the monounsaturated $'A_x/'C_x$ ions become weak in the high mass range, a feature that is also apparent in the $[M + Li]^{+}$ spectrum (Fig. 3). This phenomenon may suggest that charge-remote processes under the high-energy CID conditions used in the present work (E_{com} 200 eV) are less favourable compared to those typically observed for high-energy CID involving the use of helium as collision gas and 8 keV collisions.

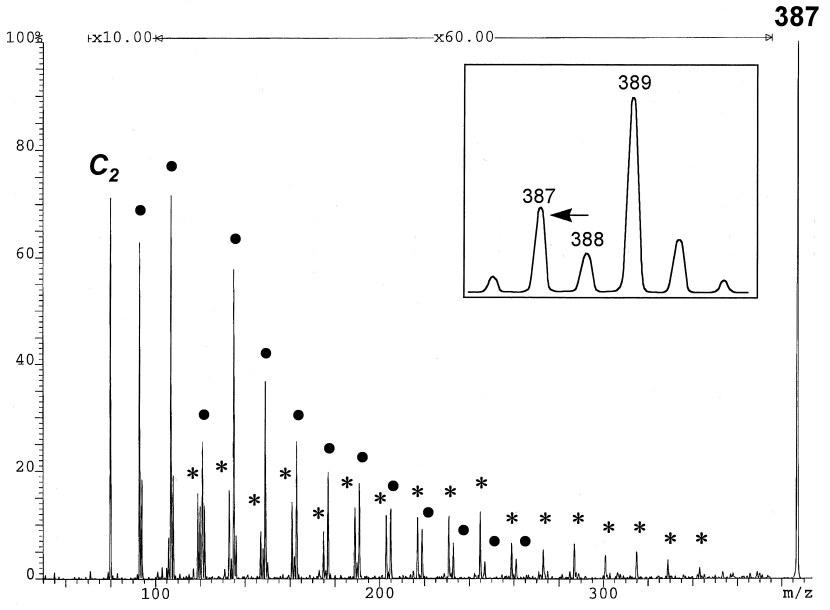

Fig. 5. High-energy CID spectrum of the methyl lignocerate $[M + Li–H_2]^+$ ion (E_{com} 200 eV). The peaks marked by ● refer to monounsaturated $'A/'C$ type ions and those marked by * to doubly unsaturated $'A/'H$ type ions. A detail of the LSI mass spectrum is given in the inset.

4.2. $[M + Na–1]^{+\bullet}$ ion structure

The high-energy CID spectra (E_{com} 200 eV) of the $[M + Na]^+$ and $[M + Na–2]^+$ ions of methyl lignocerate (not shown) were comparable to those obtained for the Li^+-cationized molecule, except that in addition to $'C_x$ type ions also C_x ions corresponding to alkyl losses were noted. The formation of C_x ions is a typical feature for $[M + Na]^+$ high-energy CID spectra, which has been discussed in detail in a recent study by Claeys et al. [15].

The low-energy CID spectrum (E_{com} 8 eV) of the $[M + Na–H]^{+\bullet}$ ion of methyl lignocerate is illustrated in Fig. 6. The product ion profile is very similar to that found for the $[M + Li–H]^{+\bullet}$] ion except that in addition to $'C_x$ ions also homologous C_x ions at masses 1 u higher are observed. As discussed already for the $[M + Li–H]^{+\bullet}$ ion, the formation of a homologous series of $'C_x$ ions indicates that hydrogen loss during cesium ion bombardment occurs at both charge-remote and charge-proximate positions of the acyl chain. The mechanism for the formation of a homologous series of C_x ions is still unclear at present. The formation of C_x ions may point to a lower initial energy deposition in the precursor $[M + Na–H]^{+\bullet}$ ion. It has been reported for functionalized alkanes by Wysocki and Ross [21] that in addition to terminally unsaturated ions corresponding to formal alkane losses, also OE ions because of alkyl losses are formed during surface-induced dissociation when the precursor ions have a low internal energy.

4.3. $[M + H–1]^{+\bullet}$ ion structure

The high-energy CID spectrum of protonated methyl lignocerate was quite different from those obtained for the Li^+- and Na^+-cationized molecules and is illustrated in Fig. 7. The spectrum is very complex and only some selected features will be discussed here. The low mass region shows ions at m/z 41, 43, 55, 57, 69, 71, and 97 consistent with the formation of carbocations that were also noticed in a previous study on high-energy CID of monoacylglycerides [17]. The ions at m/z 74, 87, and 143 are characteristic fragments of $M^{+\bullet}$ ions generated by

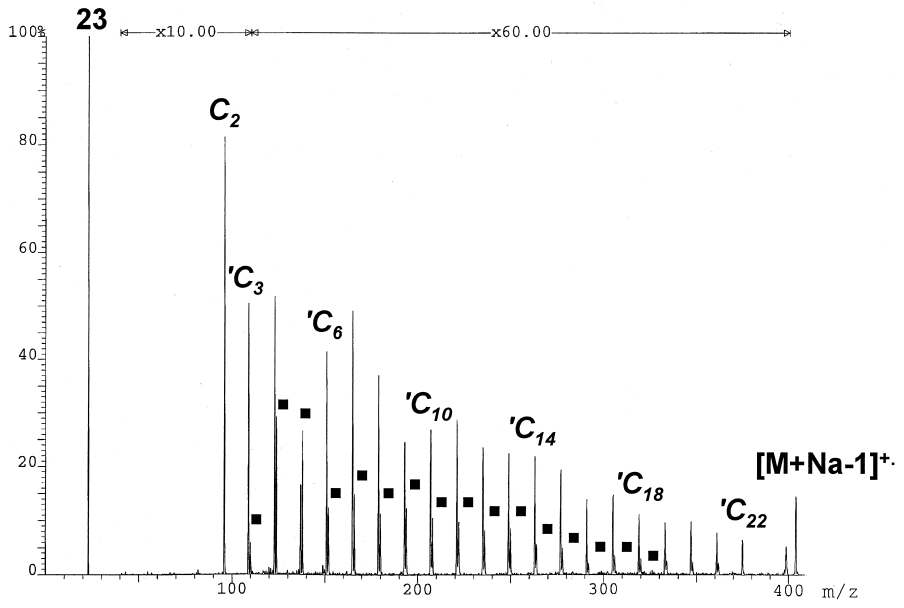

Fig. 6. Low-energy CID spectrum of the methyl lignocerate $[M + Na–H]^{+\bullet}$ ion (E_{com} 8 eV). The peaks marked by ■ refer to *C* type ions.

electron impact (EI), suggesting that during high-energy CID of $[M + H]^+$ ions a hydrogen radical is expelled from the protonated ester group. However, it is evident from the spectrum that $'C_x$ type ions are formed, suggesting that hydrogen radicals are also eliminated from charge-remote positions along the acyl chain.

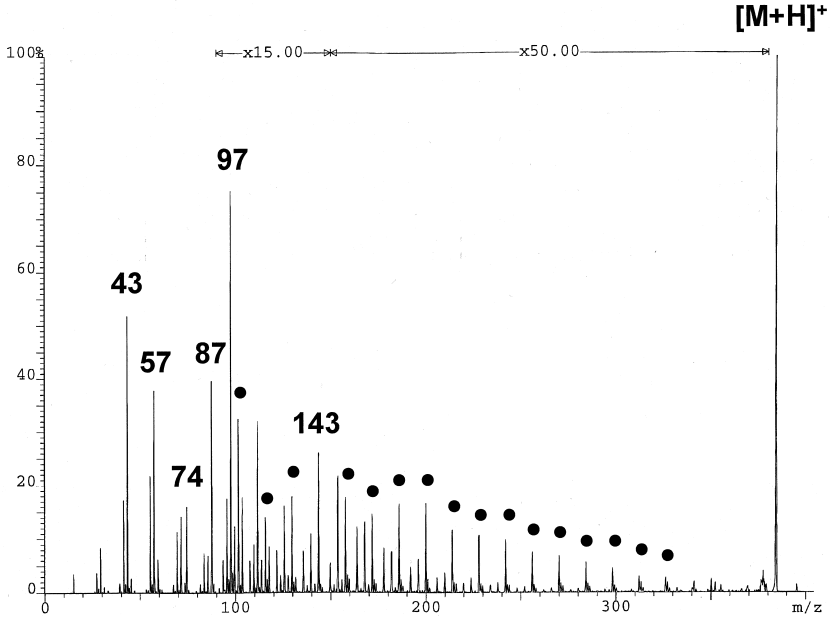

Fig. 7. High-energy CID spectrum of the methyl lignocerate $[M + H]^+$ ion (E_{com} 200 eV). $'C_x$ type ions are marked by ●.

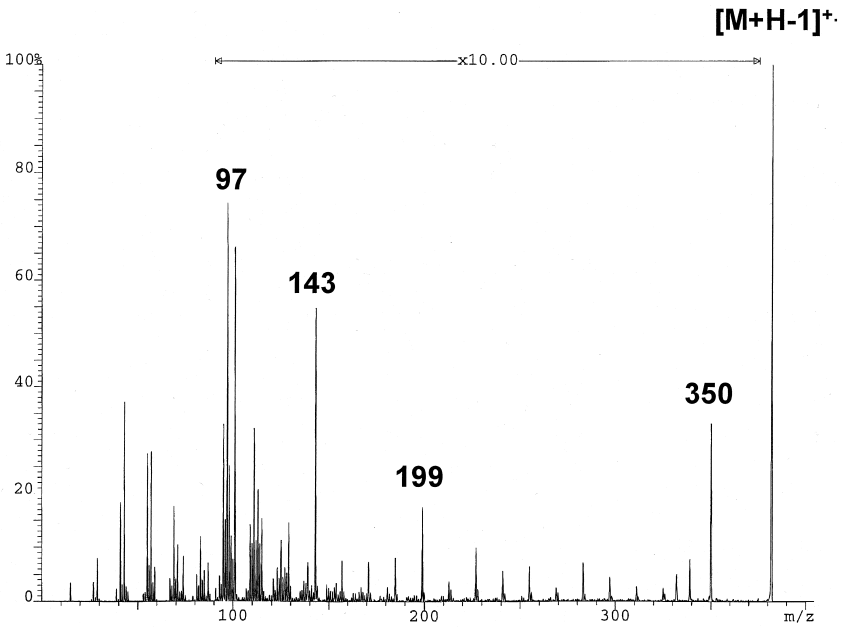

Fig. 8. High-energy CID spectrum of the methyl lignocerate $[M + H–H]^{+\bullet}$ ion (E_{com} 200 eV).

The high-energy CID spectrum of the $[M + H–H]^{+\bullet}$ or $M^{+\bullet}$ ion of methyl lignocerate formed during cesium ion bombardment is demonstrated in Fig. 8. The product ion profile is very similar to that observed for EI (Fig. 9). It is pointed out that the enhanced abundance of the carbomethoxy ions at *m*/*z*

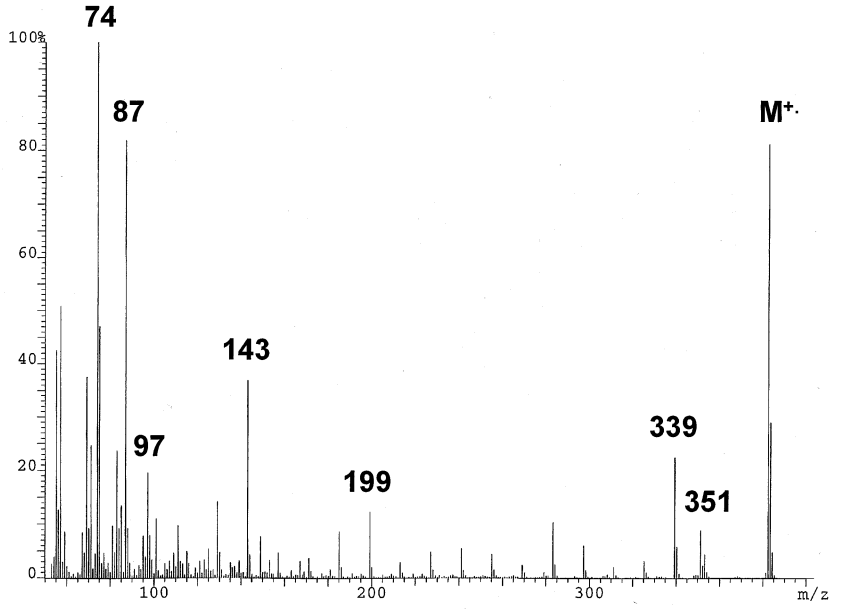

Fig. 9. EI spectrum of methyl lignocerate.

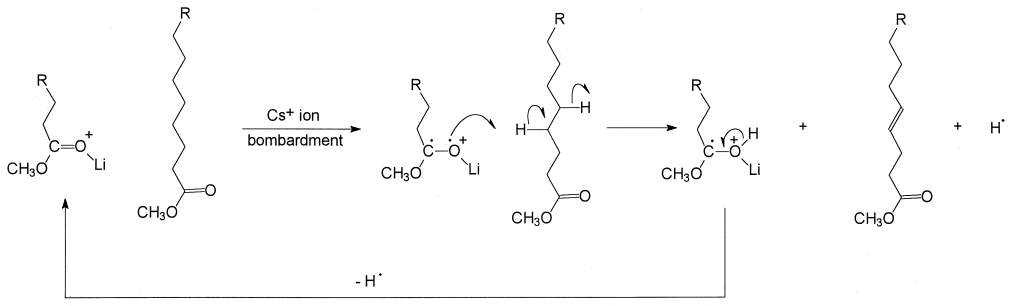

Scheme 2. Mechanism proposed for H_2 loss observed during cesium ion bombardment of Li^+-cationized fatty acid methyl esters.

143 and 199 is characteristic of the $M^{+\bullet}$ ion. Furthermore, it is worth mentioning that the ion at *m*/*z* 74 corresponding to a McLafferty rearrangement has a low abundance in the high-energy CID spectrum, a feature that has been well documented by Zirrolli and Murphy [22] for low-energy CID of fatty acid methyl ester $M^{+\bullet}$ ions. The $[M + H–H–32]^{+\bullet}$ ion at *m*/*z* 350 corresponding to the loss of methanol indicates that the $[M + H–H]^{+\bullet}$ ion population also contains species with an intact protonated ester group. Based on the observations described above it is suggested that the $[M + H–H]^{+\bullet}$ ion population consists of $M^{+\bullet}$ ions having a structure similar to that formed during EI, but additionally contains a mixture of distonic ions with a protonated ester group and a remote radical site because of hydrogen radical removal at positions all along the acyl chain.

5. Conclusion

5.1. Mechanistic considerations

In previous studies we have proposed that charge-remote fragmentation reactions in Li^+- and Na^+-cationized fatty acid methyl esters under high-energy CID conditions are initiated by a homolytic C–H cleavage that is triggered by a transient diradical formed by local excitation of the ester carbonyl group [15]. The molecular hydrogen loss observed during cesium ion bombardment of Li^+- and Na^+-cationized fatty acid methyl esters may be rationalized by a similar mechanism. Considering the fact that multiple H_2 loss occurs in case of the higher fatty acid methyl ester homologs for which the alkali metal-cationized molecules show a decreased desorption relative to the lower homologs, we believe it is reasonable to propose that the primary reaction corresponds to an intermolecular reaction between an energized alkali-cationized molecule and a neutral one [reaction (1)]. Following cationization the neutral $[M–H_2]$ species formed in this primary reaction is detectable at 2 u lower than the $[M + Li]^+$ ion [reaction (2)], whereas the $[M + Li + H]^{+\bullet}$ ion may undergo loss of $H^\bullet$ in a radical-induced reaction leading to regeneration of the ester carbonyl bond [reaction (3)].

$$[M + Li]^+ + M \rightarrow [M + Li + H]^{+\bullet} + [M–H_2] + H^\bullet \quad (1)$$

$$[M - H_2] + Li^+ \rightarrow [M + Li–H_2]^+ \quad (2)$$

$$[M + Li + H]^{+\bullet}–H^\bullet \rightarrow [M + Li]^+ \quad (3)$$

A plausible mechanism for the primary reaction (1) and for reaction (3) is suggested in Scheme 2.

The inhibitory effect of unsaturation and branching can be understood considering the proposed mechanism: unsaturation may give rise to competitive hydrogen and alkyl radical loss resulting in stabilized allylic radical species, whereas branching likely influences this process in a steric manner.

The ion structures of the methyl lignocerate $[M + Li/Na–H]^{+\bullet}$ ion reveal that hydrogen radical removal for Li^+- and Na^+-cationized molecules under cesium ion bombardment is different from that observed for

the protonated molecule where a hydrogen radical is also expelled from the protonated ester group. No obvious tendency for an enhanced loss of H_2 could be found with increasing acyl chain length for protonated fatty acid methyl esters, suggesting that alkali metal cationization is important in the dehydrogenation chemistry.

The present study also provides information on the phase in which molecular hydrogen removal takes place. The sample-to-*m*-NBA cluster ratios for comparable amounts of fatty acid methyl esters were found to be dependent upon the acyl chain length and indicate that the desorption of alkali metal-cationized molecules from the condensed phase worsens for the higher homologs examined. The increased tendency of higher fatty acid methyl ester homologs to undergo fast ion-beam-induced reactions may be related to a different physical state of the analyte/matrix mixture in the surface region, more specifically, to a more viscous, glassy state [23,24]. It has been demonstrated that a highly viscous state, as caused by a high surface concentration of analyte molecules, raises the energy transfer to molecules and ions in the sputtering process leading to a decreased molecular ion intensity and increased fragmentation and chemical noise.

Acknowledgements

This work was supported by the Fund for Scientific Research (FWO-Flanders) through grant no. 6.0082.98. M. Claeys is indebted to the FWO as a research director. L. Nizigiyimana is on leave from the University of Burundi and thanks the Belgian Ministry of Foreign Affairs (ABOS) for a doctoral research fellowship. We wish to thank Dr. J. Pugh of Micromass for recording spectra on the AutoSpec oaTof mass spectrometer. Professor F.W. Röllgen of the University of Bonn (D) is gratefully acknowledged for useful comments.

References

[1] L. Nizigiyimana, H. Van den Heuvel, M. Claeys, J. Mass Spectrom. 32 (1997) 277.
[2] J. Claereboudt, W. Baeten, H. Geise, M. Claeys, Org. Mass Spectrom. 28 (1993) 71.
[3] G.R. Fenwick, J. Eagles, R. Self, Biomed. Mass Spectrom. 10 (1983) 382.
[4] G. Allmaier, E.R. Schmid, H. Gasser, W. Strohmaier, G. Schlag, Rapid Commun. Mass Spectrom. 4 (1990) 19.
[5] C.E. Heine, M.M. Geddes, Org. Mass Spectrom. 29 (1994) 277.
[6] G. Klesper, F.W. Röllgen, J. Mass Spectrom. 31 (1996) 383.
[7] M. Takayama, T. Fukai, T. Nomura, K. Nojima, Rapid Commun. Mass Spectrom. 3 (1989) 4.
[8] R.T. Rosen, T.G. Hartman, J.D. Rosen, C.-T. Ho, Rapid Commun. Mass Spectrom. 2 (1988) 21.
[9] O. Curcuroto, P. Traldi, G. Moneti, L. Corda, G. Podda, Org. Mass Spectrom. 26 (1991) 713.
[10] G.J.C. Paul, R. Feng, M.J. Bertrand, Int. J. Mass Spectrom. Ion Processes 145 (1995) 123.
[11] G.J.C. Paul, S. Bourg, M.J. Bertrand, J. Am. Soc. Mass Spectrom. 4 (1993) 493.
[12] J.F. Van Bocxlaer, M. Claeys, H. Van den Heuvel, A.P. De Leenheer, J. Mass Spectrom. 30 (1995) 69.
[13] W.J. Griffiths, Y. Yang, J.A. Lindgren, J. Sjövall, Rapid Commun. Mass Spectrom. 10 (1996) 21.
[14] M. Claeys, L. Nizigiyimana, H. Van den Heuvel, P.J. Derrick, Rapid Commun. Mass Spectrom. 10 (1996) 770.
[15] M. Claeys, L. Nizigiyimana, H. Van den Heuvel, I. Vedernikova, A. Haemers, J. Mass Spectrom. 33 (1998) 631.
[16] J. Adams, Mass Spectrom. Rev. 9 (1990) 141.
[17] R.H. Bateman, M.R. Green, G. Scott, Rapid Commun. Mass Spectrom. 9 (1995) 1227.
[18] N.J. Jensen, K.B. Tomer, M.L. Gross, J. Am. Chem. Soc. 107 (1995) 1863.
[19] L. Nizigiyimana, H. Van den Heuvel, M. Claeys, J. Mass Spectrom. and Rapid Commun. Mass Spectrom., Special volume, Proceedings of the 3rd International Symposium on Applied Mass Spectrometry in the Health Sciences and the European Tandem Mass Spectrometry Conference, Barcelona, 9–13 July, 1995, p. S19.
[20] M. Claeys, H. Van den Heuvel, Biol. Mass Spectrom. 23 (1994) 20.
[21] V.H. Wysocki, M.M. Ross, Int. J. Mass Spectrom. Ion Processes 104 (1991) 179.
[22] J.A. Zirrolli, R.C. Murphy, J. Am. Soc. Mass Spectrom. 4 (1993) 223.
[23] S.S. Wong, F.W. Röllgen, I. Manz, M. Przybylski, Biomed. Mass Spectrom. 12 (1985) 43.
[24] E. Junker, K.P. Wirth, F.W. Röllgen, Int. J. Mass Spectrom. Ion Processes 122 (1992) 3.